Optical control of magnetization and spin blockade in graphene quantum dots

A. D. Güçlü and P. Hawrylak

Quantum Theory Group, Security and Disruptive Technology, Emerging Technologies Division, National Research Council of Canada, Ottawa, Canada and Department of Physics, University of Ottawa, Ottawa, Canada

(Received 11 July 2012; published 23 January 2013)

We show that the magnetization of triangular graphene quantum dots with zigzag edges can be manipulated optically. When the system is charge neutral, the magnetic moment can be first erased by addition of a single electron spin with a gate, then restored by absorption of a photon. The conversion of a single photon to a magnetic moment results in a many-body effect, optical spin blockade. The effect demonstrated here can potentially lead to efficient spin to photon conversion, quantum memories, and single-photon detectors.

DOI: 10.1103/PhysRevB.87.035425 PACS number(s): 73.22.−f, 73.22.Pr, 78.67.−n, 85.75.−d

Graphene quantum dots[1–31] offer the possibility of integrating electronic, photonic, and magnetic functionalities in a single material, carbon, realizing a long standing goal of semiconductor spintronics.[32,33] Without external doping or spin injection[34] but rather through edge, shape, and size engineering, graphene quantum dots are predicted to exhibit a finite magnetic moment while retaining good electronic and optical properties.[17–22]

At present, silicon is the material of choice for electronics, compound semiconductors for optoelectronics and photonics, and ferromagnets for memory. The integration of these different functionalities is the goal of semiconductor spintronics,[32,33] which attempts to exploit the spin of the electron in addition to its charge. This requires either efficient spin injection and detection,[34] or doping of semiconductors with magnetic ions.[32,33] In semiconductors doped with Mn ions, ferromagnetism can be controlled with gate voltage by controlling carrier density.[33] However, the doping responsible for ferromagnetism leads to the degradation of optical properties. On the other hand, graphene, when reduced in size to a nanoscale island, has an energy gap tunable by the size from terahertz to UV.[21] The zigzag edge of graphene quantum dot leads to a shell of degenerate states in the middle of the gap between valence and conduction bands. In particular, in triangular graphene quantum dots (TGQDs) where all the edge atoms belong to the same sublattice, Coulomb interactions among electrons occupying the half-filled degenerate shell lead to a finite magnetic moment.[23–31] Since the shell filling can be controlled by the gate, so are the optical transitions from the filled valence band to the degenerate shell allowing for the gate tunable optical and magnetic properties.[21,27] Here, we show that in TGQDs it is possible to optically control the magnetization through optical spin blockade and hence convert a photon to a magnetic moment.

Figure 1 schematically shows the process of optical manipulation of the magnetic moment S, total spin, in a TGQD with zigzag edges. The blue balls illustrate carbon atoms held together by sp^2 bonds, and red arrows illustrate p_z electron spin density. When the TGQD is charge neutral [Fig. 1(a)] electrons in the vicinity of zigzag edges align their spin through exchange interaction, giving rise to a net magnetic moment S. If the TGQD is charged with a single additional electron by a gate, the added electron must have spin opposite to the magnetization S [Fig. 1(b)]. Through electron-electron interactions, electrons attempt to align their spin with the added electron, inducing spin depolarization as illustrated in Fig. 1(c). However, the spin polarization can be recovered by absorption of a single photon. The absorbed photon creates a hole in the valence band (thick arrow) and an electron in the degenerate shell at zero-energy Fermi level, as shown in Fig. 1(d). The exchange interaction between the valence hole and all the electrons in the degenerate shell aligns the spin of electrons in the degenerate shell and restores the magnetic moment [Fig. 1(e)]. Hence one can erase the magnetic moment with a gate and restore it optically. It is thus possible to control the magnetization of a graphene quantum dot with zigzag edges through optical spin blockade.

We now briefly describe the theoretical model and computational details that underlie the optical spin blockade. We consider a TGQD with zigzag edges and N carbon atoms as shown in Fig. 1. We use an effective tight-binding Hamiltonian $H_{\rm TB} = \sum_{i,l,\sigma} t_{il} c^{\dagger}_{i\sigma} c_{l\sigma}$ for a single electron on carbon p_z orbitals, where the operator $c^{\dagger}_{i\sigma}$ creates a p_z electron on site "i" with spin σ. The hopping terms t_{il} are taken to be $t = -2.5$ eV for nearest neighbors and $t' = -0.1$ eV for next-nearest neighbours. Edge atoms are assumed to be passivated by a single hydrogen atom. The stability of zigzag edges passivated by hydrogen atoms was previously established theoretically[29] and recently confirmed experimentally.[35] We illustrate our theory on the example of TGQD with $N = 97$ atoms, the single particle spectrum of which, obtained by diagonalization of the one-electron Hamiltonian, is shown in Fig. 2(a) (left panel). As discussed already,[21,23–27] there exists a shell of degenerate states at the Fermi level (zero-energy states) with degeneracy N_d, where N_d is the number of atoms at one edge minus one,[28] $N_d = 7$ in Fig. 2(a). In the zero-energy shell the number of electrons N_e equals the number of zero-energy states N_d. The exchange interaction aligns the spin of all electrons. This is schematically illustrated in Fig. 2(a) by placing an arrow in each state of the degenerate shell. With the zero-energy shell partially occupied, optical transitions from valence to zero-energy band can occur,[21] with oscillator strength determined by dipole moments $|\langle i|\mathbf{r}|j\rangle|^2$ where j is the valence-band state, and i is a zero-energy state.

In the remainder of the discussion we will be charging the TGQD with additional electrons from a nearby metallic gate. As discussed in Ref. 27, we first empty the zero-energy shell and perform Hartree-Fock calculation for doubly occupied

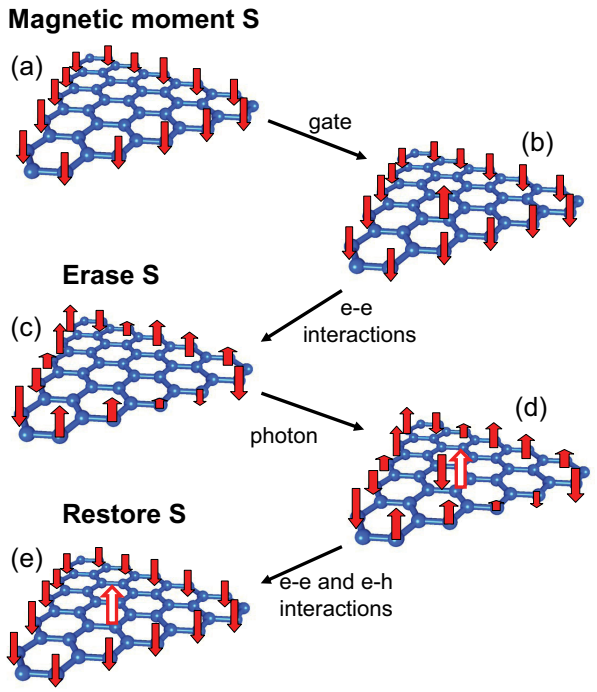

FIG. 1. (Color online) Schematic illustration of optical control of magnetization and origin of optical spin blockade: Creation of magnetic moment S; erasure of S with addition of a single electron, which through e-e interactions destroys S; restoration of S by absorption of a single photon that creates an exciton, which restores magnetic moment S through e-e and e-h interactions.

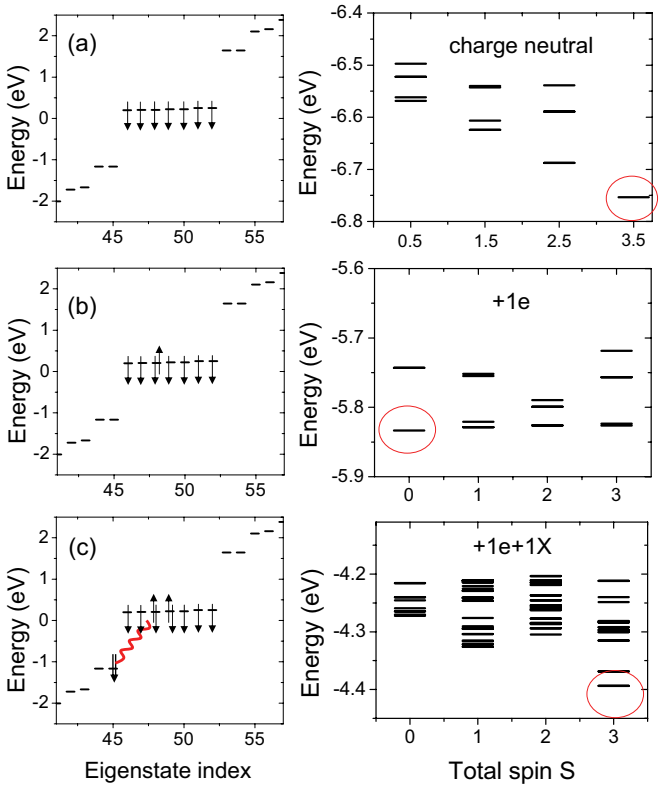

FIG. 2. (Color online) Noninteracting (left panels) and many-body (right panels) energy spectra showing the ground-state total spin of (a) charge neutral, (b) charged, and (c) charged and photoexcited quantum dot with seven zero-energy states.

valence states separated by energy gap from empty zero-energy and conduction band states. Once the self-consistent Hartree-Fock quasiparticle levels $|q\rangle$ for valence and $|p\rangle$ for zero-energy states are obtained, we proceed with rotating the original interacting electron Hamiltonian to the basis of quasi-electrons in the zero-energy shell interacting with holes in the valence band,

$$\begin{aligned} H = & \sum_{p,\sigma} \epsilon_p b^\dagger_{p\sigma} b_{p\sigma} + \sum_{p,\sigma} \epsilon_q h^\dagger_{q\sigma} h_{q\sigma} \\ & + \frac{1}{2} \sum_{\substack{pqrs \\ \sigma\sigma'}} \langle pq|V|rs\rangle b^\dagger_{p\sigma} b^\dagger_{q\sigma'} b_{r\sigma'} b_{s\sigma} \\ & + \frac{1}{2} \sum_{\substack{pqrs \\ \sigma\sigma'}} \langle pq|V|rs\rangle h^\dagger_{p\sigma} h^\dagger_{q\sigma'} h_{r\sigma'} h_{s\sigma} \\ & - \sum_{\substack{pqrs \\ \sigma\sigma'}} (\langle rp|V|sq\rangle - (1-\delta_{\sigma\sigma'})\langle rp|V|qs\rangle) \\ & \times b^\dagger_{p\sigma} h^\dagger_{q\sigma'} h_{r\sigma'} b_{s\sigma}, \end{aligned} \tag{1}$$

where $b^\dagger_{p\sigma}$ ($h^\dagger_{q\sigma}$) creates an electron (hole) in the Hartree-Fock state $|p\rangle$ ($|q\rangle$).

Next, we construct a basis of all configurations corresponding to a given number of electrons N_e in the zero-energy shell and holes N_h in the valence band, build a Hamiltonian matrix in the space of configurations, and diagonalize the matrix to obtain eigenstates and eigenenergies of the interacting electron-hole system.

The left panel of Fig. 2(a) shows the single-particle energy levels of a noninteracting TGQD. The arrows schematically show a single configuration of $N_e = 7$ quasi-electrons with all electron spins aligned. The total spin S of this spin polarized configuration is $S = 7/2$. There are many other configurations possible with total spin varying from $S = 7/2$ to $S = 1/2$. The low-energy spectra for the charge neutral TGQD for different possible total spin S are shown in Fig. 2(a), right panel. We see that the ground state, indicated by a circle, indeed corresponds to a maximally spin-polarized state with $S = 3.5$. Hence neutral TGQD carries a magnetic moment as shown in Fig. 1(a).

Figure 2(b) shows the effect of the additional electron on single-particle (left) and many-particle (right) spectrum of TGQD. In a single-particle spectrum, an additional electron is added to the spin-polarized configuration, also shown in Fig. 1(b). This electron has a spin opposite to the total spin of the TGQD. Such configuration has a total spin of $S = 7/2 - 1/2 = 3$. Figure 2(b), right panel, shows the low-energy spectrum of the interacting system. The ground state, marked with a circle, has instead a total spin $S = 0$. Addition of a single electron erased the magnetic moment of a TGQD, as was illustrated in Fig. 1(c) and discussed earlier in Ref. 27. It has been recently shown that the erasure of the magnetic moment by a single charge is possible up to a critical size of TGQD.[30] The robustness of spin depolarization and its stability against

temperature is controlled by the energy gaps shown in the energy diagram of Fig. 2(b). These energy gaps are controlled by e-e interactions alone. The magnitude depends on the size and inversely on the dielectric screening. Reducing the size from $N = 97$ (Fig. 2) to $N = 22$ atoms increases the energy gap to 20 meV. Reducing screening from $\kappa = 6$ (Fig. 2) to $\kappa = 1$ increases the energy gap from 5meV (Fig. 2) to 30 meV.

Figure 2(c) shows the effect of absorption of a single photon in a charged TGQD of Fig. 2(b). In the left panel, noninteracting single-particle states are shown. The photoexcited configuration consists of a spin-polarized shell, one additional electron with opposite spin and a photoexcited opposite spin electron and a hole in the valence band, i.e., an exciton X. The right panel of Fig. 2(c) shows the low-energy spectrum of the interacting electron-hole system. We see that the ground state corresponds to total spin $S = 6/2$. Since the optically excited exciton X is in a singlet state, i.e., does not carry net spin, the ground-state total spin $S = 6/2$ corresponds to a configuration shown in Fig. 1(b) and left panel of Fig. 2(b). Hence addition of exciton to the charged TGQD restored the maximally polarized state. We can understand this remarkable effect as follows. When the system is photoexcited, a valence electron is transferred into the zero-energy shell leaving a hole behind. The addition of an extra electron to the strongly correlated spin $S = 0$ state does not change the spin polarization, resulting in a $S = 1/2$ spin-depolarized ground state, as shown in Fig. 3. However, if this additional electron is accompanied by the valence hole, a significant rearrangement of electronic correlations takes place. The introduction of the valence hole spin maximizes the exchange energy between the valence hole and electrons in a degenerate zero-energy shell only if they have aligned spins. Hence there is a competition between electronic correlations in the charged degenerate shell, which destroy spin polarization and exchange interaction with the valence hole, which favor the spin-polarized state. Exact diagonalization of the interacting electron system shows that the exchange with the valence hole wins and, as a result, for optically excited system, the total spin is maximized: the electron total spin is $S_e = |N_d - 2|/2$ due to the two extra spins in the zero-energy shell. Since the valence hole total spin is $S_h = -1/2$, the net spin of the system is given by $S = |N_d - 1|/2$ ($S = 3$ in our example).

The maximal spin polarization of the photoexcited TGQD is observed not only at filling factor $\nu = 1$ but at all filling factors. Figure 3 shows the calculated ground-state total electronic spin S_e of TGQD as a function of the number of electrons (top) and filling fraction ν of the zero-energy shell. The black curve shows the total spin of the initial state and the red curve shows the total spin after absorption of a photon, i.e., with exciton X. Without the exciton, away from charge neutrality, depolarization occurs for one added electron, $\nu = (N_d + 1)/N_d = 8/7$, and for two added electrons, $\nu = (N_d + 2)/N_d = 9/7$. By contrast, the zero-energy shell after illumination is spin polarized at all filling factors. Blue and red arrows show the difference between the total spin of the initial and final photoexcited states. The blue arrow corresponds to spin difference equal to a single-electron spin while the red arrow points to a larger difference. As we demonstrate below,

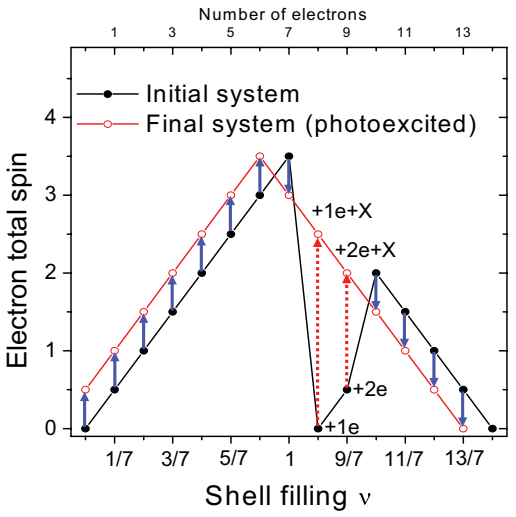

FIG. 3. (Color online) Ground-state total spin as a function of filling of the zero-energy band of the system described in Fig. 2, with and without optical activation. Magnetization of the system is stabilized by the presence of an exciton. Optically allowed and blockaded transitions are shown with blue and red arrows, respectively.

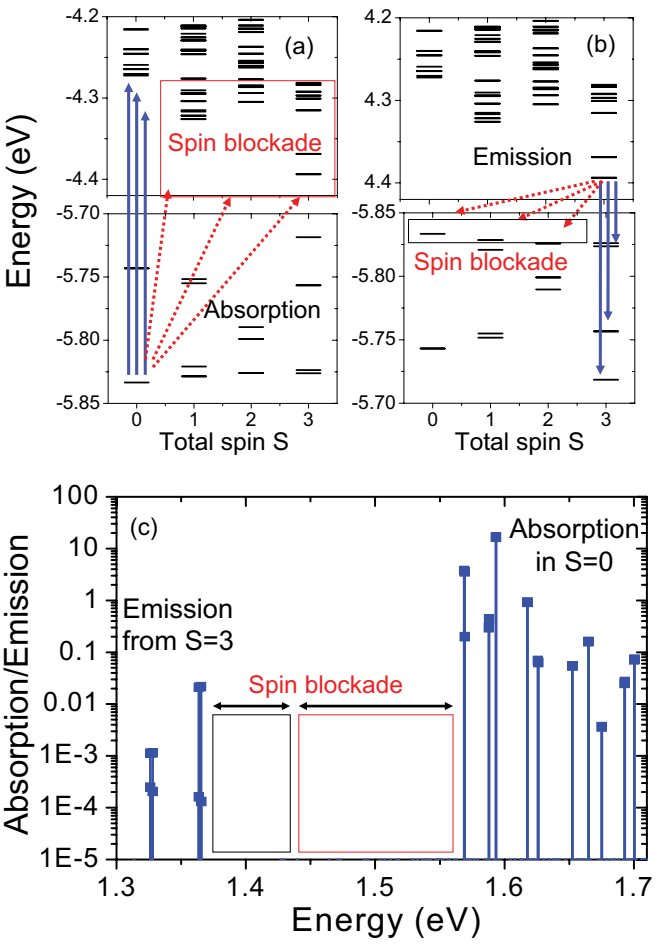

FIG. 4. (Color online) Allowed and blockaded optical transitions due to spin conservation rule in (a) the absorption and (b) emission many-body spectra. Corresponding absorption and emission lines are shown in (c).

the large spin difference between the initial and final states, shown by red dashed arrows in Fig. 3., causes an optical spin blockade in absorption and emission spectra.

The spectral function $A(\omega)$ describing annihilation of a photon and addition of exciton to a TGQD

$$A(\omega) = \sum_f |\langle M^f | P^\dagger | M^i \rangle|^2 \delta[\omega - (E_f - E_i)] \qquad (2)$$

involves transitions between the initial many-body state $|M^i\rangle$ and all final states $|M^f\rangle$ connected by the polarization operator $P^\dagger = \sum \delta_{\sigma\bar{\sigma}'} \langle p|\mathbf{r}|q\rangle b^\dagger_{p\sigma'} h^\dagger_{q\sigma}$, creating an electron in the zero-energy shell and a hole in the valence band. The many-body matrix element contains a term $< f, N_e + 1, S^f_e | b^\dagger_{p\sigma} | S^i_e, N_e, i >$ in which an electron with spin $\sigma = \pm 1/2$ in a single-particle state p is added to N_e electrons in the initial many-body state i with total spin S^i_e. The resulting $N_e + 1$ state with spin $S = S^i_e \pm 1/2$ must have a finite overlap with final state with total spin S^f_e. The overlap is finite if the total spin difference between initial and final many-body states equals the spin of one added electron. The computed spin difference between the initial and final states in the absorption process is shown with arrows in Fig. 3. Blue arrows correspond to allowed transitions with spin difference of $1/2$, while blocked transitions are shown as red arrows.

We now discuss the effect of optical spin blockade on the exciton addition and emission spectra. Figures 4(a) and 4(b) show blocked (red arrows) and allowed (blue solid arrows) optical transitions during the absorption and subsequent emission processes for TGQD charged with a single electron [Figs. 2(b) and 2(c)]. Since the ground state has a total spin $S = 0$ [Fig. 2(b)] and photon creates a singlet exciton, final states must have $S = 0$ [Fig. 4(a)]. The TGQD containing an exciton will relax to its ground state, which from Fig. 2(c) has total spin $S = 3$. The emission from the ground state with $S = 3$ to ground state with $S = 0$ is also spin blockaded, thus the system will go through optical transitions ending with excited states with $S = 3$. As a result, the absorption and emission spectra are shifted, as shown in Fig. 4(c), where the lowest energy absorption occurs at around 1.57 eV, while the lowest emission line occurs around 1.37 eV. The resulting shift between the emission and absorption spectra, 0.2 eV in this example, is a direct measure of e-e and e-h interactions and should be experimentally measurable.

In conclusion, while in a doped triangular graphene quantum dot depolarization occurs due to electron-electron interactions, the magnetization can be recovered by absorption of a photon due to electron-hole interactions. The conversion of the photon to a magnetic moment results in a many-body optical spin blockade that can be observed in absorption and emission spectra. Hence, we have demonstrated optical control of magnetization through spin blockade in graphene quantum dots, which can potentially lead to efficient spin-to-photon conversion, quantum memories, and single-photon detectors.

The authors thank P. Potasz for discussions and the Natural Sciences and Engineering Research Council, National Research Council of Canada, and the Canadian Institute for Advanced Research for support.

[1] P. R. Wallace, Phys. Rev. **71**, 622 (1947).
[2] A. H. C. Neto, F. Guinea, N. M. R. Peres, K. S. Novoselov, and A. K. Geim, Rev. Mod. Phys. **81**, 109 (2009).
[3] K. S. Novoselov, A. K. Geim, S. V. Morozov, D. Jiang, Y. Zhang, S. V. Dubonos, I. V. Grigorieva, and A. A. Firsov, Science **306**, 666 (2004).
[4] Y. B. Zhang, Y. W. Tan, H. L. Stormer, and P. Kim, Nature (London) **438**, 201 (2005).
[5] M. L. Sadowski, G. Martinez, M. Potemski, C. Berger, and W. A. de Heer, Phys. Rev. Lett. **97**, 266405 (2006).
[6] L. Yang, M. L. Cohen, and S. G. Louie, Phys. Rev. Lett. **101**, 186401 (2008).
[7] J. Jung and A. H. MacDonald, Phys. Rev. B **79**, 235433 (2009).
[8] L. Brey and H. A. Fertig, Phys. Rev. B **73**, 235411 (2006).
[9] J. Wurm, A. Rycerz, I. Adagideli, M. Wimmer, K. Richter, and H. U. Baranger, Phys. Rev. Lett. **102**, 056806 (2009).
[10] K. A. Ritter and J. W. Lyding, Nature Mater. **8**, 235 (2009).
[11] S. Schnez, F. Molitor, C. Stampfer, J. Güttinger, I. Shorubalko, T. Ihn, and K. Ensslin, Appl. Phys. Lett. **94**, 012107 (2009).
[12] I. Deretzis, G. Forte, A. Grassi, A. La Magna, G. Piccitto, and R. Pucci, J. Phys.: Condens. Matter. **22**, 0955 (2010).
[13] Y. Morita, S. Suzuki, K. Sato, and T. Takui, Nature Chem. **3**, 197 (2011).
[14] J. Lu, P. S. E. Yeo, C. K. Gan, P. Wu, and K. P. Loh, Nature Nanotechnol. **6**, 247 (2011).
[15] D. Subramaniam, F. Libisch, Y. Li, C. Pauly, V. Geringer, R. Reiter, T. Mashoff, M. Liebmann, J. Burgdorfer, C. Busse, T. Michely, R. Mazzarello, M. Pratzer, and M. Morgenstern, Phys. Rev. Lett. **108**, 046801 (2012).
[16] M. Olle, G. Ceballos, D. Serrate, and P. Gambardella, Nano Lett. **12**, 4431 (2012).
[17] Z. Z. Zhang, K. Chang, and F. M. Peeters, Phys. Rev. B **77**, 235411 (2008).
[18] M. L. Mueller, X. Yan, J. A. McGuire, and L. Li, Nano Lett. **10**, 2679 (2010).
[19] X. Yan, X. Cui, B. S. Li, and L. S. Li, Nano Lett. **10**, 1869 (2010).
[20] Y. Li, Y. Hu, Y. Zhao, G. Shi, L. Deng, Y. Hou, and L. Qu, Adv. Mater. **23**, 776 (2011).
[21] A. D. Güçlü, P. Potasz, and P. Hawrylak, Phys. Rev. B **82**, 155445 (2010).
[22] Juan Peng, Wei Gao, Bipin Kumar Gupta, Zheng Liu, Rebeca Romero-Aburto, Liehui Ge, Li Song, Lawrence B. Alemany, Xiaobo Zhan, Guanhui Gao, Sajna Antony Vithayathil, Benny Abraham Kaipparettu, Angel A. Marti, Takuya Hayashi, Jun-Jie Zhu, and Pulickel M. Ajayan, Nano Lett. **12**, 844 (2012).
[23] M. Ezawa, Phys. Rev. B **76**, 245415 (2007).
[24] J. Fernández-Rossier and J. J. Palacios, Phys. Rev. Lett. **99**, 177204 (2007).

[25]J. Akola, H. P. Heiskanen, and M. Manninen, Phys. Rev. B **77**, 193410 (2008).
[26]W. L. Wang, S. Meng, and E. Kaxiras, Nano Lett. **8**, 241 (2008).
[27]A. D. Güçlü, P. Potasz, O. Voznyy, M. Korkusinski, and P. Hawrylak, Phys. Rev. Lett. **103**, 246805 (2009).
[28]P. Potasz, A. D. Güçlü, and P. Hawrylak, Phys. Rev. B **81**, 033403 (2010).
[29]O. Voznyy, A. D. Güçlü, P. Potasz, and P. Hawrylak, Phys. Rev. B **83**, 165417 (2011).
[30]P. Potasz, A. D. Güçlü, A. Wojs, P. Hawrylak, Phys. Rev. B **85**, 075431 (2012).
[31]H. Sahin, R. T. Senger, and S. Ciraci, J. Appl. Phys. **108**, 074301 (2010).
[32]T. Dietl, Nat. Mater. **9**, 965 (2010).
[33]M. Ohno, D. Chiba, F. Matsukura, T. Omiya, E. Abe, T. Dietl, Y. Ohno, and T. Ohtani, Nature (London) **408**, 944 (2000).
[34]G. Kioseoglou, M. Yasar, C.H. Li, M. Korkusinski, M. Diaz-Avila, A.T. Hanbicki, P. Hawrylak, A. Petrou, and B.T. Jonker, Phys. Rev. Lett. **101**, 227203 (2008).
[35]X. Zhang, O. V. Yazyev, J. Feng, L. Xie, C. Tao, Y.-C. Chen, L. Jiao, Z. Pedramrazi, A. Zettl, S. G. Louie, H. Dai, and M. F. Crommie, ACS Nano (2012).